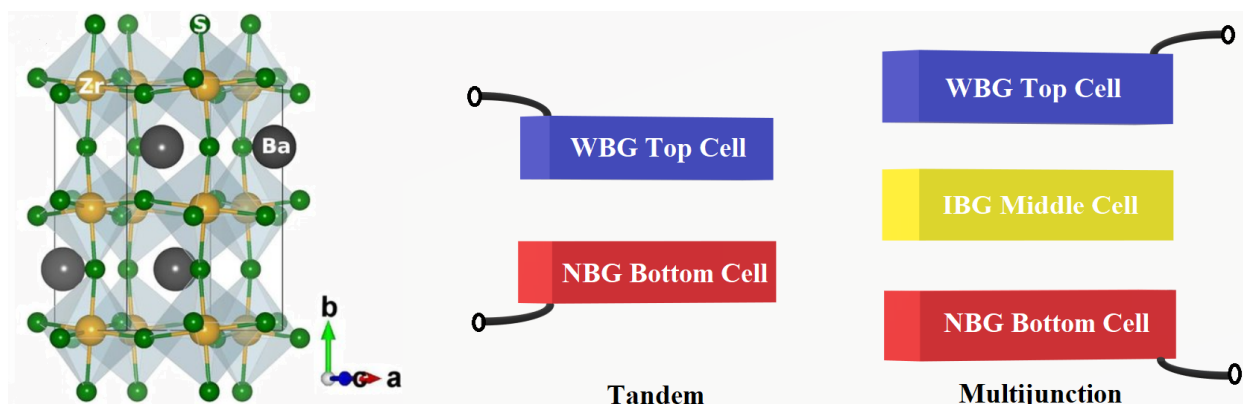


Barium Zirconium Sulphide Chalcogenide Perovskites for Lead-free Tandem and Multijunction Perovskite Photovoltaics

Dinesh Behera



INTRODUCTION

In Photovoltaics, a theoretical radiative limit exists on the single junction absorbers, which predicts a maximum power conversion efficiency (PCE) of 33.7%, which happens for a bandgap energy value of about 1.34 eV.¹ This limit on the PCE arises due to short circuit current (J_{SC}) losses (transmission and thermalization losses), open circuit voltage (V_{OC}) deficit (recombination losses), and fill factor (FF) losses (parasitic resistance losses).² However, a method helpful in overcoming the limit on the PCE by minimizing the J_{SC} losses by stacking multiple light-absorbing layers with complementary bandgaps. Such devices are the tandem solar cell devices (two junctions (2J)) and the multijunction solar cell devices (3J or more).³

III-V compound semiconductors-based multijunction solar cells based on GaAs and GaInP, have proven their remarkable potential in 2J, 3J, and 4J solar cell devices by achieving PCEs of about 31%, 38%, and 39%, respectively, under standard terrestrial conditions.⁴ Despite these achievements, the manufacturing processes required for these crystalline, lattice-matched multijunction solar cells, such as metal-organic chemical vapour deposition (MOCVD) or molecular beam epitaxy (MBE), remain exceptionally expensive. This cost challenge hinders the widespread deployment of such high-performance solar cells in terrestrial applications.

Perovskites, on the other hand, with ABX_3 crystal form, because of their tunable bandgap⁵, cost-effective facile fabrication, high efficiency, defect tolerance, high specific power (power per

weight)⁶, and excellent radiation tolerance⁷, are promising absorbers in tandem and multijunction solar cell devices.⁸ These exciting features of perovskites make them attractive for space applications as well. The selection of the A = (Cs, MA or FA), B = (Sn or Pb), and X = (I, Br or Cl) can tune the bandgap from 1.2 eV to 3.5 eV.⁹ This feature is the most important for their applications in tandem and triple junction solar cells. The work by Maximilian T. Hörantner et al. has shown that perovskite-based tandem and multi-junction devices have the potential to break the records set by the III-V semiconductors-based tandem and multijunction solar cells.⁸

The narrow bandgap (NBG) absorbers for bottom cells in tandem and multijunction devices are well-established as wafer-based crystalline silicon (1.12 eV bandgap)¹⁰, and thin-film-based CIGS ($\text{CuIn}_{1-x}\text{Ga}_x\text{Se}_2$, with x tuning the bandgap from 1.0 to 1.7 eV)¹¹. For all perovskites-based tandem and multijunction devices, mixed Sn/Pb perovskites have the potential to reach near their thermodynamic limit for V_{OC} .¹² The intermediate bandgap (typically 1.6 eV) absorbers in the multijunction devices are plenty and well-established as the standard methylammonium lead iodide (MAPI) as well as other mixed-cation mixed-halide-based perovskites.¹³ Lead-based I/Br mixed-halide perovskites ($\text{APb}(\text{I}_{1-x}\text{Br}_x)_3$), on increasing x, exhibit bandgaps ranging from 1.5 to 2.4 eV.¹⁴ Hence, based on the bandgap range, these mixed-halide perovskites make the appropriate wide bandgap (WBG) absorbers in tandem and multijunction devices.

However, the quest for suitable bandgap faces complexities in terms of unstable compositions, and thereby the WBG absorbers have yet to achieve comparable success in PCE as their bottom cell counterparts. The low PCEs of WBG solar cells are attributed to the V_{OC} losses¹⁴ arising from light-induced phase segregation or halide segregation (also known as the Hoke effect).¹⁵ Halide segregation takes place in mixed-halide perovskite films, resulting in the development of iodide-rich and bromide-rich phases. These iodide-rich phases exhibit lower bandgaps than the surrounding material, hence pinning down the V_{OC} of the solar cell.¹⁴ Efforts are underway to address this issue, and while progress has been made in mitigating the problem, there is still room for improvement. For instance, the most recent work on suppressing halide segregation by compositional engineering of Cs-based inorganic I/Br mixed-halide perovskites has been demonstrated by Zaiwei Wang et al., and their work suggests that increasing lattice distortion in the perovskites by compositional engineering is positively correlated to the suppression of phase segregation.¹⁶ While their device demonstrates notable resistance to phase segregation, further comprehensive studies are necessary to facilitate its practical implementation in wide bandgap devices.

As Bingcheng Yu et al. suggest inorganic perovskite materials showcase higher thermal and light illumination stabilities than hybrid organic-inorganic perovskites¹⁷, as well as for the need of the hour to reduce the dependence on lead-based perovskite materials, the material scientists have suggested the use of a new class of materials, the inorganic lead-free chalcogenide perovskite materials.^{18,19} One of the most promising materials in this subset is the barium zirconium sulphide (BaZrS_3), which shows an inherent bandgap of 1.8-1.9 eV, a high absorption coefficient of the order of 10^5 cm^{-1} and greater, high carrier mobilities, high thermal stability, and high defect tolerance.^{18,20,21} The inherent bandgap along with the superior optoelectronic

properties of BaZrS_3 place them at par with the absorbers qualifying for the top cell in tandem and multijunction devices.

THE POTENTIAL OF BaZrS_3 PHOTOVOLTAICS

Drift-diffusion-based device simulations are based on the numerical simulations and analysis of the basic equations for a p-n junction diode, which include Poisson's equations, transport equations, and continuity equations for charge carriers.^{22,23} Such a device simulation study of a BaZrS_3 -based WBG solar cell device (with TiO_2 as the electron transport layer (ETL) and Cu_2O as the hole transport layer (HTL)) by S. Karthick et al. has shown promising PCE of about 12.5% along with a high V_{OC} of 1.2 V.²⁴ Similar work by Hend I. Alkhamash and M. M. Haque have demonstrated 17.1% PCE and a V_{OC} of 1.0 V.²⁵ This high performance sets them as attractive absorbers for the top cell in tandem and multijunction devices.

Further, research efforts focused on bandgap tuning to creating intermediate bandgap absorbers have yielded thin films of $\text{BaZr}_{1-x}\text{Ti}_x\text{S}_3$ (1.4-1.6 eV bandgap) and $\text{BaZr}(\text{S}_{1-x}\text{Se}_x)_3$ (1.4-1.76 eV bandgap).^{26,27} The above-mentioned work by S. Karthick et al. also simulates 1.63 eV $\text{BaZr}_{1-x}\text{Ti}_x\text{S}_3$ and 1.76 eV $\text{BaZr}(\text{S}_{1-x}\text{Se}_x)_3$ which yielded PCEs of 18.9% and 15.5% respectively with an approximately similar V_{OC} of 1.2 V.²⁴ This suggests that these absorbers have the potential to replace the lead-based intermediate bandgap counterparts.

Furthermore, a similar device simulation work by Nikhil Thakur et al. has simulated an NBG BaZrSe_3 (1.01 eV bandgap) absorber-based solar cell device and demonstrated a PCE of about 19.2%.²⁸ Correspondingly, this suggests that this new absorber can be a potential bottom cell choice. Hence, this opens up the possibility of all-lead-free inorganic chalcogenide perovskites-based tandem and multijunction solar cells.

CHALLENGES FOR BaZrS_3 PHOTOVOLTAIC DEVICES

BaZrS_3 is thermally stable for around 600C²⁹ and hence requires a crystallisation temperature of >600C. The early work on physical vapour deposition (PVD) techniques like Sputtering and Pulsed Laser Deposition (PLD) have confirmed the deposition of thin films of BaZrS_3 by sulphurisation at high temperatures of nearly 1000C.^{21,30-32} High-quality epitaxial growth of lattice-matched BaZrS_3 thin films by molecular beam epitaxy (MBE) also calls for high temperatures of 900C.³³ These techniques have hence confirmed the high-temperature crystallization of the BaZrS_3 films making the standard solar cell device architecture difficult to realise as the predeposited transport layers (TLs) and the substrate transparent conductive oxide (TCO) layers tend to evaporate and degrade at such high temperatures.³⁴ The issue of bottom layers evaporating at its crystallization temperature further hinders the potential of this material in tandem and multijunction solar cell devices. There have been attempts to tackle this issue in terms of the work on low-temperature solution-based thin film deposition by Vikash Kumar Ravi et al. and Daniel Zilevu et al. suggest taking the route of colloidal nanomaterials or nanocrystals.^{35,36} However, the crystallinity and the thermal stability of the material are reduced significantly in the low-temperature colloidal solution methods, which can reduce the performance of the perovskite absorber and which is undesirable. The work by Corrado

Comparotto et al. instills hope for sputtering and PLD by introducing SnS-capped Ba-Zr precursors which sulphurise at around 600C.³⁷ However, more research is needed in this domain. All of the above-mentioned reasons necessitate the search for high-temperature compatible bottom layers. However, tandem and multijunction applications would require more meticulous and extensive research in terms of bottom-layer materials. This serves as a major setback and is evident by a little to no amount of work in this area.

FUTURE POSSIBILITIES FOR BaZrS₃ PHOTOVOLTAIC DEVICES

Promising prospects emerge for this lead-free inorganic chalcogenide-based perovskite material, particularly with the advent of new device architectures. These architectures enable the deposition of TCO layers and TLs after applying the perovskite film on thermally stable substrates such as glass, Si, or SiC. Referred to as all-back contact architectures, these designs have already proven successful in crystalline silicon solar cells and are now being adapted for perovskite solar cells.^{38–40} Rear contact solar cells were originally proposed and used for silicon wafer-based solar cells to reduce the shading by contacts for achieving higher efficiencies. However, this is now being implemented and used for perovskite solar cells.⁴¹ Among these rear contact architectures, the interdigitated back contact (IBC) architecture stands out as the most promising. In IBC architecture, the rear side of the solar cell features an interdigitated arrangement of metal contacts, forming alternating fingers of n-type and p-type contacts. Implementation of such architectures often involves advanced techniques such as photolithography and e-beam lithography. However, photolithography and e-beam lithography are cost-ineffective, and sophisticated technologies. For perovskite solar cells, to tackle this situation, in 2022, low-cost honeycomb electrode-based IBC architectures were proposed by Siqi Deng et al. and Kevin J. Prince et. al. via microsphere lithography, and cracked film lithography, respectively.^{42,43} In 2023, Jonathon Harwell et al. successfully demonstrated an IBC architecture of honeycomb-patterned electrodes via low-cost nanoimprint lithography for perovskite solar cells.⁴⁴ These advancements signify a pivotal step forward in the realm of BaZrS₃ chalcogenide perovskite-based solar cell device fabrication. They not only mark progress but also unlock promising avenues for potential breakthroughs, particularly in the application of these devices in tandem and multijunction configurations.

CONCLUSION

The adoption of the IBC architecture holds promise in advancing research to unlock the remarkable potential of BaZrS₃ for tandem and multijunction devices. This progress necessitates a meticulous selection of materials to mitigate parasitic absorption and thin film interference effects in tandem and multijunction devices.⁸ The strategic choice of materials becomes crucial for optimising the performance of these devices and harnessing the full capabilities of BaZrS₃. Anticipated progress is towards the realization of an all-lead-free chalcogenide perovskite tandem and multijunction solar cell. The advancement of such environmentally friendly, efficient, and stable solar cell technologies not only holds great promise for the future of sustainable energy on Earth but also opens possibilities for applications beyond our planet in extraterrestrial environments.

REFERENCES

- ¹ W. Shockley, and H.J. Queisser, "Detailed Balance Limit of Efficiency of p-n Junction Solar Cells," *J. Appl. Phys.* **32**(3), 510–519 (2004).
- ² H.J. Queisser, "Detailed balance limit for solar cell efficiency," *Mater. Sci. Eng. B* **159–160**, 322–328 (2009).
- ³ M. Yamaguchi, F. Dimroth, J.F. Geisz, and N.J. Ekins-Daukes, "Multi-junction solar cells paving the way for super high-efficiency," *J. Appl. Phys.* **129**(24), 240901 (2021).
- ⁴ M.A. Green, E.D. Dunlop, M. Yoshita, N. Kopidakis, K. Bothe, G. Siefer, and X. Hao, "Solar cell efficiency tables (version 62)," *Prog. Photovolt. Res. Appl.* **31**(7), 651–663 (2023).
- ⁵ J. Albero, A. M. Asiri, and H. García, "Influence of the composition of hybrid perovskites on their performance in solar cells," *J. Mater. Chem. A* **4**(12), 4353–4364 (2016).
- ⁶ Y. Tu, J. Wu, G. Xu, X. Yang, R. Cai, Q. Gong, R. Zhu, and W. Huang, "Perovskite Solar Cells for Space Applications: Progress and Challenges," *Adv. Mater.* **33**(21), 2006545 (2021).
- ⁷ F. Lang, G.E. Eperon, K. Frohna, E.M. Tennyson, A. Al-Ashouri, G. Kourkafas, J. Bundesmann, A. Denker, K.G. West, L.C. Hirst, H.-C. Neitzert, and S.D. Stranks, "Proton-Radiation Tolerant All-Perovskite Multijunction Solar Cells," *Adv. Energy Mater.* **11**(41), 2102246 (2021).
- ⁸ M.T. Hörantner, T. Leijtens, M.E. Ziffer, G.E. Eperon, M.G. Christoforo, M.D. McGehee, and H.J. Snaith, "The Potential of Multijunction Perovskite Solar Cells," *ACS Energy Lett.* **2**(10), 2506–2513 (2017).
- ⁹ G.E. Eperon, M.T. Hörantner, and H.J. Snaith, "Metal halide perovskite tandem and multiple-junction photovoltaics," *Nat. Rev. Chem.* **1**(12), 1–18 (2017).
- ¹⁰ E. Aydin, E. Ugur, B.K. Yildirim, T.G. Allen, P. Dally, A. Razzaq, F. Cao, L. Xu, B. Vishal, A. Yazmaciyan, A.A. Said, S. Zhumagali, R. Azmi, M. Babics, A. Fell, C. Xiao, and S. De Wolf, "Enhanced optoelectronic coupling for perovskite/silicon tandem solar cells," *Nature* **623**(7988), 732–738 (2023).
- ¹¹ A. Maoucha, H. Ferhati, F. Djeflal, and F. AbdelMalek, "Highly efficient Cd-Free ZnMgO/CIGS solar cells via effective band-gap tuning strategy," *J. Comput. Electron.* **22**(3), 887–896 (2023).
- ¹² J. Tong, Z. Song, D.H. Kim, X. Chen, C. Chen, A.F. Palmstrom, P.F. Ndione, M.O. Reese, S.P. Dunfield, O.G. Reid, J. Liu, F. Zhang, S.P. Harvey, Z. Li, S.T. Christensen, G. Teeter, D. Zhao, M.M. Al-Jassim, M.F.A.M. van Hest, M.C. Beard, S.E. Shaheen, J.J. Berry, Y. Yan, and K. Zhu, "Carrier lifetimes of $>1\ \mu\text{s}$ in Sn-Pb perovskites enable efficient all-perovskite tandem solar cells," *Science* **364**(6439), 475–479 (2019).
- ¹³ R. Prasanna, A. Gold-Parker, T. Leijtens, B. Conings, A. Babayigit, H.-G. Boyen, M.F. Toney, and M.D. McGehee, "Band Gap Tuning via Lattice Contraction and Octahedral Tilting in Perovskite Materials for Photovoltaics," *J. Am. Chem. Soc.* **139**(32), 11117–11124 (2017).
- ¹⁴ S. Mahesh, J.M. Ball, R.D.J. Oliver, D.P. McMeekin, P.K. Nayak, M.B. Johnston, and H.J. Snaith, "Revealing the origin of voltage loss in mixed-halide perovskite solar cells," *Energy Environ. Sci.* **13**(1), 258–267 (2020).
- ¹⁵ E.T. Hoke, D.J. Slotcavage, E.R. Dohner, A.R. Bowring, H.I. Karunadasa, and M.D. McGehee, "Reversible photo-induced trap formation in mixed-halide hybrid perovskites for photovoltaics," *Chem. Sci.* **6**(1), 613–617 (2014).

- ¹⁶ Z. Wang, L. Zeng, T. Zhu, H. Chen, B. Chen, D.J. Kubicki, A. Balvanz, C. Li, A. Maxwell, E. Ugur, R. dos Reis, M. Cheng, G. Yang, B. Subedi, D. Luo, J. Hu, J. Wang, S. Teale, S. Mahesh, S. Wang, S. Hu, E.D. Jung, M. Wei, S.M. Park, L. Grater, E. Aydin, Z. Song, N.J. Podraza, Z.-H. Lu, J. Huang, V.P. Dravid, S. De Wolf, Y. Yan, M. Grätzel, M.G. Kanatzidis, and E.H. Sargent, "Suppressed phase segregation for triple-junction perovskite solar cells," *Nature* **618**(7963), 74–79 (2023).
- ¹⁷ B. Yu, S. Tan, D. Li, and Q. Meng, "The stability of inorganic perovskite solar cells: from materials to devices," *Mater. Futur.* **2**(3), 032101 (2023).
- ¹⁸ D. Tiwari, O.S. Hutter, and G. Longo, "Chalcogenide perovskites for photovoltaics: current status and prospects," *J. Phys. Energy* **3**(3), 034010 (2021).
- ¹⁹ S. Perera, H. Hui, C. Zhao, H. Xue, F. Sun, C. Deng, N. Gross, C. Milleville, X. Xu, D.F. Watson, B. Weinstein, Y.-Y. Sun, S. Zhang, and H. Zeng, "Chalcogenide perovskites – an emerging class of ionic semiconductors," *Nano Energy* **22**, 129–135 (2016).
- ²⁰ M. Kumar, A. Singh, D. Gill, and S. Bhattacharya, "Optoelectronic Properties of Chalcogenide Perovskites by Many-Body Perturbation Theory," *J. Phys. Chem. Lett.* **12**(22), 5301–5307 (2021).
- ²¹ X. Wei, H. Hui, C. Zhao, C. Deng, M. Han, Z. Yu, A. Sheng, P. Roy, A. Chen, J. Lin, D.F. Watson, Y.-Y. Sun, T. Thomay, S. Yang, Q. Jia, S. Zhang, and H. Zeng, "Realization of BaZrS₃ chalcogenide perovskite thin films for optoelectronics," *Nano Energy* **68**, 104317 (2020).
- ²² P.A. Basore, "Numerical modeling of textured silicon solar cells using PC-1D," *IEEE Trans. Electron Devices* **37**(2), 337–343 (1990).
- ²³ M. Burgelman, P. Nollet, and S. Degraeve, "Modelling polycrystalline semiconductor solar cells," *Thin Solid Films* **361–362**, 527–532 (2000).
- ²⁴ S. Karthick, S. Velumani, and J. Bouclé, "Chalcogenide BaZrS₃ perovskite solar cells: A numerical simulation and analysis using SCAPS-1D," *Opt. Mater.* **126**, 112250 (2022).
- ²⁵ H.I. Alkhamash, and M.M. Haque, "Device modelling and performance analysis of chalcogenide perovskite-based solar cell with diverse hole transport materials and back contact metals," *Jpn. J. Appl. Phys.* **62**(1), 012006 (2023).
- ²⁶ S. Sharma, Z. Ward, K. Bhimani, K. Li, A. Lakhnot, R. Jain, S.-F. Shi, H. Terrones, and N. Koratkar, "Bandgap Tuning in BaZrS₃ Perovskite Thin Films," *ACS Appl. Electron. Mater.* **3**(8), 3306–3312 (2021).
- ²⁷ H. Zitouni, N. Tahiri, O. El Bounagui, and H. Ez-Zahraouy, "Electronic, optical and transport properties of perovskite BaZrS₃ compound doped with Se for photovoltaic applications," *Chem. Phys.* **538**, 110923 (2020).
- ²⁸ N. Thakur, P. Kumar, and P. Sharma, "Simulation study of chalcogenide perovskite (BaZrSe₃) solar cell by SCAPS-1D," *Mater. Today Proc.*, (2023).
- ²⁹ S. Niu, J. Milam-Guerrero, Y. Zhou, K. Ye, B. Zhao, B.C. Melot, and J. Ravichandran, "Thermal stability study of transition metal perovskite sulfides," *J. Mater. Res.* **33**(24), 4135–4143 (2018).
- ³⁰ C. Comparotto, A. Davydova, T. Ericson, L. Riekehr, M.V. Moro, T. Kubart, and J. Scragg, "Chalcogenide Perovskite BaZrS₃: Thin Film Growth by Sputtering and Rapid Thermal Processing," *ACS Appl. Energy Mater.* **3**(3), 2762–2770 (2020).
- ³¹ S.P. Ramanandan, A. Giunto, E.Z. Stutz, B. Reynier, I.T.F.M. Lefevre, M. Rusu, S. Schorr, T. Unold, A.F.I. Morral, J.A. Márquez, and M. Dimitrievska, "Understanding the growth mechanism of BaZrS₃ chalcogenide perovskite thin films from sulfurized oxide precursors," *J. Phys. Energy* **5**(1), 014013

(2023).

³² J.A. Márquez, M. Rusu, H. Hempel, I.Y. Ahmet, M. Kölbach, I. Simsek, L. Choubrac, G. Gurieva, R. Gunder, S. Schorr, and T. Unold, "BaZrS₃ Chalcogenide Perovskite Thin Films by H₂S Sulfurization of Oxide Precursors," *J. Phys. Chem. Lett.* **12**(8), 2148–2153 (2021).

³³ I. Sadeghi, K. Ye, M. Xu, Y. Li, J.M. LeBeau, and R. Jaramillo, "Making BaZrS₃ Chalcogenide Perovskite Thin Films by Molecular Beam Epitaxy," *Adv. Funct. Mater.* **31**(45), 2105563 (2021).

³⁴ M.S. Farhan, E. Zalnezhad, A.R. Bushroa, and A.A.D. Sarhan, "Electrical and optical properties of indium-tin oxide (ITO) films by ion-assisted deposition (IAD) at room temperature," *Int. J. Precis. Eng. Manuf.* **14**(8), 1465–1469 (2013).

³⁵ V.K. Ravi, S.H. Yu, P.K. Rajput, C. Nayak, D. Bhattacharyya, D.S. Chung, and A. Nag, "Colloidal BaZrS₃ chalcogenide perovskite nanocrystals for thin film device fabrication," *Nanoscale* **13**(3), 1616–1623 (2021).

³⁶ D. Zilevu, O.O. Parks, and S.E. Creutz, "Solution-phase synthesis of the chalcogenide perovskite barium zirconium sulfide as colloidal nanomaterials," *Chem. Commun.* **58**(75), 10512–10515 (2022).

³⁷ C. Comparotto, P. Ström, O. Donzel-Gargand, T. Kubart, and J.J.S. Scragg, "Synthesis of BaZrS₃ Perovskite Thin Films at a Moderate Temperature on Conductive Substrates," *ACS Appl. Energy Mater.* **5**(5), 6335–6343 (2022).

³⁸ E.V. Kerschaver, and G. Beaucarne, "Back-contact solar cells: a review," *Prog. Photovolt. Res. Appl.* **14**(2), 107–123 (2006).

³⁹ K. Yoshikawa, H. Kawasaki, W. Yoshida, T. Irie, K. Konishi, K. Nakano, T. Uto, D. Adachi, M. Kanematsu, H. Uzu, and K. Yamamoto, "Silicon heterojunction solar cell with interdigitated back contacts for a photoconversion efficiency over 26%," *Nat. Energy* **2**(5), 1–8 (2017).

⁴⁰ E. Franklin, K. Fong, K. McIntosh, A. Fell, A. Blakers, T. Kho, D. Walter, D. Wang, N. Zin, M. Stocks, E.-C. Wang, N. Grant, Y. Wan, Y. Yang, X. Zhang, Z. Feng, and P.J. Verlinden, "Design, fabrication and characterisation of a 24.4% efficient interdigitated back contact solar cell," *Prog. Photovolt. Res. Appl.* **24**(4), 411–427 (2016).

⁴¹ W. Yang, Z. Yang, C. Shou, J. Sheng, B. Yan, and J. Ye, "Optical design and optimization for back-contact perovskite solar cells," *Sol. Energy* **201**, 84–91 (2020).

⁴² S. Deng, B. Tan, A.S.R. Chesman, J. Lu, D.P. McMeekin, Q. Ou, A.D. Scully, S.R. Raga, K.J. Rietwyk, A. Weissbach, B. Zhao, N.H. Voelcker, Y.-B. Cheng, X. Lin, and U. Bach, "Back-contact perovskite solar cell fabrication via microsphere lithography," *Nano Energy* **102**, 107695 (2022).

⁴³ K.J. Prince, C.P. Muzzillo, M. Mirzokarimov, C.A. Wolden, and L.M. Wheeler, "All-Back-Contact Perovskite Solar Cells Using Cracked Film Lithography," *ACS Appl. Energy Mater.* **5**(8), 9273–9279 (2022).

⁴⁴ J. Harwell, and I.D.W. Samuel, "Nanoimprint Lithography as a Route to Nanoscale Back-Contact Perovskite Solar Cells," *ACS Appl. Nano Mater.* **6**(16), 14940–14947 (2023).